

Comparison of Optical Sparse Aperture Image Restoration with Experimental PSF and Designed PSF

Zhiwei Zhou, Dayong Wang

Applied Science, Beijing University of Technology, Beijing, 100124, P.R.China

Juan Zhao, Yuhong Wan, Zhuqing Jiang, Shiquan Tao

Applied Science, Beijing University of Technology, Beijing, 100124, P.R.China

Abstract

The digital post-processing method is needed to restore the image quality from the blurring image output directly from optical sparse aperture imaging systems. The common method for post-processing is the Wiener filter, where the important parameter is the point spread function (PSF). The Wiener filter will deconvolve the convolution effect if the PSF is the precise impulse response of the optical sparse aperture system. Usually it is hard to measure the PSF experimentally. On the contrary, it is easy to calculate the PSF based on telescope array configuration, which is given by design. In order to evaluate whether the calculated PSF is adaptable to the image restoration, a comparison of the image restoration has been done by using these two kinds of PSFs. The results show that the calculated PSF works well in the case that the co-phasing error is small, while the measured PSF is ineffective.

Key words: sparse aperture; Wiener filter; PSF

1. Introduction

With the exploration of outer space getting deeper, a high angular resolution telescope is necessary to study the specific structure of universe, however, the quest for high angular resolution telescope inevitably leads to large aperture, which is limited by the volume and mass constrain of current launch vehicles as well as the financial support limitation[1][2]. Since the difficulty of manufacturing a large diameter monolithic prime mirror telescope increases rapidly, the optical sparse aperture telescope is proposed to resolve this problem.

An optical sparse aperture telescope consists of several independent small telescopes, each of that will collect light separately. This structure is called Fizeau interferometry telescope, which is also called Image-plane interferometry because it is the method of combining multiple beams, each focused to make an image of the sky. Since the Fizeau interferometers produce direct images with full spatial frequency coverage, and only the light collection areas decreases, the picture obtained from the optical sparse aperture telescope needs post-processing to retrieve the original image of the sky.

The mostly common method used for the image restoration of the optical sparse aperture telescope is the Wiener filter in the spatial frequency domain [3]. The most important parameter of the Wiener filter is the optical transfer function (OTF) which is the Fourier transformation of point spread function (PSF). There are two possible ways to obtain the OTF of the system. Both methods are in need of PSF first. One method calculates the Fourier transformation of designed aperture function, named the calculated PSF. Another method detects experimentally the PSF by using a CCD, when the system is illuminated with the quasi-monochromatic light. Such PSF is named the measured PSF, which is usually considered to be the practical PSF of system. However, it is difficult to measure the PSF of optical sparse aperture telescope with large aperture. Although there are some alternate methods, the measurement of PSF is still difficult. On the contrary, the calculated PSF is very easy to obtain through the Fourier transformation. In this paper, we present an analysis and an comparison of the image restoration with these two PSFs of the optical sparse aperture system, and demonstrate the feasibility of the calculated PSF and the measured PSF respectively.

2. Theory of imaging and image restoration

The imaging process of the optical sparse aperture systems can be simplified to be incoherent optical system described with the Eq.(1).

$$i(x_f, y_f) = i_g(x_f, y_f) * PSF(x_f, y_f) + n(x_f, y_f) \quad 1$$

where the ‘*’ is convolution operand, $i(x_f, y_f)$ stands for the light intensity distribution of image plane, $i_g(x_f, y_f)$ is the light intensity distribution of the geometrical ideal image, $PSF(x_f, y_f)$ is the point spread function of system, and $n(x_f, y_f)$ is the noise distribution. According to the Eq. (1), if the $PSF(x_f, y_f)$ is known, the geometrical ideal image can be retrieved through the deconvolution process.

The PSF of an optical sparse aperture system is the square of modulus of Fourier transformation of system exit pupil, as shown in Eq. (2):

$$PSF(x_f, y_f) = |\mathfrak{F}[P(x, y)]|^2 \quad 2$$

which is called the impulse response[4]. Because the exit beam of each sub-telescope is still parallel, the system exit pupil is determined by sub-telescope array configuration [5]. There are three major types of telescope array configurations: Tri-Arm, Golay and Annulus.

The digital image restoration is based on Wiener filter in the frequency domain. OTF which is the Fourier transformation of PSF is the most important parameter in Wiener filter as shown in Eq.(3a) and Eq.(3b). $W(f_x, f_y)$ is the Wiener filter expression in frequency domain, $N(f_x, f_y)$ is the noise spectrum and $\tilde{I}_g(f_x, f_y)$ is the spectrum of the geometrical ideal image. Here the ‘*’ is complex conjugate operand. In fact, since the $N(f_x, f_y)$ is usually unknown, a constant K is used for substitute of $|N(f_x, f_y)| / \tilde{I}_g(f_x, f_y)^2$. f is the distance from the exit pupil to the image plane. The Wiener filter essence is an inverse filter, if the constant K equals zero.

$$W(f_x, f_y) = \frac{OTF^*(f_x, f_y)}{|OTF(f_x, f_y)|^2 + |N(f_x, f_y)| / \tilde{I}_g(f_x, f_y)^2} \quad 3a$$

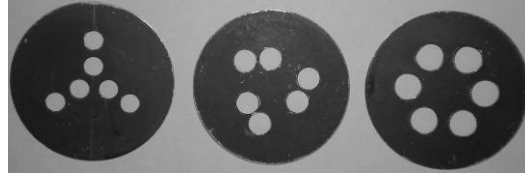
$$OTF(f_x, f_y) = \mathfrak{F}[PSF(x_f, y_f)]_{f_x = \frac{x}{\lambda f}, f_y = \frac{y}{\lambda f}} \quad 3b$$

3. Measured and Calculated PSF

The PSF of the optical sparse aperture imaging system is obtained from two main ways: experiment and calculation [6].

1) Measured PSF

Because the input and output beam are both parallel, the telescope array configuration is simplified to a pupil mask as shown in Fig.1. These pupil masks are the exit pupil function of the system. The Fig.2 shows our experimental setup for the measurement of PSF [7]. A pinhole with a diameter of 10 μ m, is used to simulate a point source. The pinhole was put in the forward focal plane of the achromatic doublet lens L_1 so as to produce parallel lights. The mask is placed in front of the achromatic doublet lens L_2 , and the CCD was put at the focal plane of the L_2 . The lenses of L_1 and L_2 are set to be as close as possible. The image captured by the CCD is the pattern of the Fourier transformation of the mask’s transmission function, which is the PSF of the system.



(a) Tri-Arm (b) Golay-6 (c) Annulus

Fig.1 Masks used in the experiments

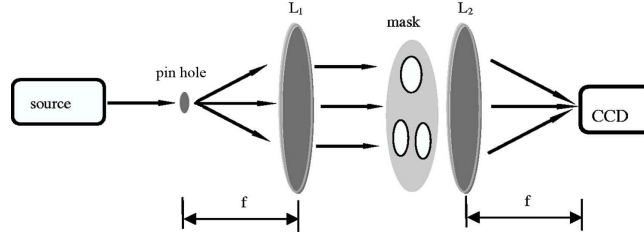


Fig.2 Setup for the measurement of the PSF

2) Calculated PSF

The PSF can also be calculated from the exit pupil function. The array pupil function $P(x,y)$ is demonstrated in Eq.(4) [8]:

$$P(x, y) = \sum_{n=1}^N P(x - a_n, y - b_n) e^{j\phi_n(x,y)} \quad 4$$

where a_n, b_n are the central coordinates of a sub-telescope, and $\phi_n(x,y)$ is the phase error of the nth aperture. Supposed the phase error changes little, the $\phi_n(x,y)$ is simplified to a constant ϕ_n . Eq.(5) is the PSF of an optical sparse aperture system with phase error:

$$PSF(x_f, y_f) = PSF_{sub}(x_f, y_f) \times \left\{ \left[N + 2 \sum_{k=1}^{N(N+1)/2} \cos[2\pi(\Delta x_k x_f + \Delta y_k y_f + \Delta \phi_k)] \right] \right\} \quad 5$$

$\Delta x_k, \Delta y_k$ are the vector separation components between pairs of sub-aperture centers, $\Delta \phi_k$ is the phase difference between pairs of sub-aperture, λ is the wavelength, and f is the distance from the pupil to the image plane.

Eq.(6) reveals the OTF of the sparse aperture system with little phase error:

$$OTF(f_x, f_y) = OTF_{sub}(f_x, f_y) * \left[\delta(f_x, f_y) + \frac{1}{N} \sum_{k=1}^{N(N+1)/2} \delta\left(f_x \pm \frac{\Delta x_k}{\lambda f}, f_y \pm \frac{\Delta y_k}{\lambda f}\right) \times \exp\left(-j2\pi\Delta \phi_k \left(\frac{f_x}{\Delta x_k} + \frac{f_y}{\Delta y_k}\right)\right) \right] \quad 6$$

where ‘*’ is the convolution operand.

4. Experimental results

1) Results of the calculated PSF

According to the experimental setup shown in Fig.2, $f = 840\text{mm}$, the central wavelength is 532nm , and the CCD valid area is 1317×1035 . The sampling interval of CCD is $6.8\mu\text{m} \times 6.8\mu\text{m}$ with a nominally linear 12 bit response. The explicit parameters of pupil masks are included in Table 1, and their calculated PSFs are shown in Fig.3.

Table 1 the explicit parameters of three type's masks

	Sub-aperture diameter (mm)	Equivalent filled aperture diameter (mm)	Filled Factor
Tri-Arm	6.4	35	20.06%
Golay-6	7.8	35	29.80%
Annulus	9.0	35	39.67%

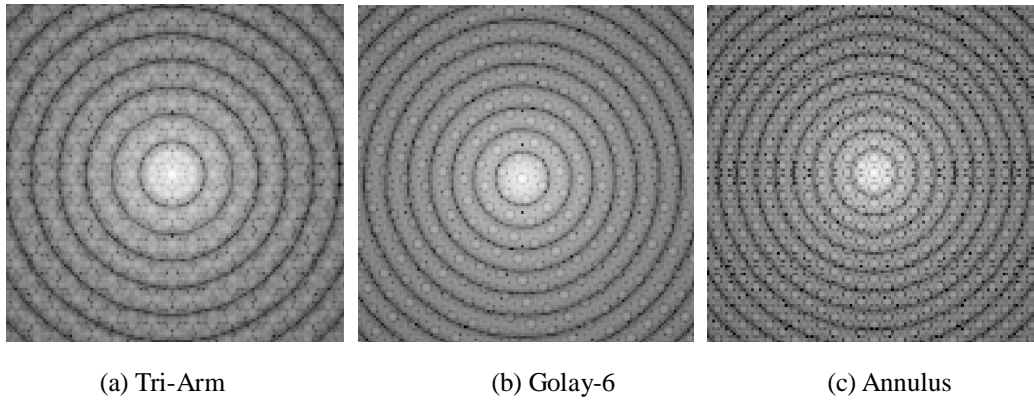


Fig.3 The calculated PSFs of three typical array configurations

2) Results of the measured PSF

The PSF images captured by the CCD are shown in Fig.4, where the system is illuminated by a 532nm diode laser. In order to obtain the incoherent light, a random phase plate is put in the front of the pinhole.

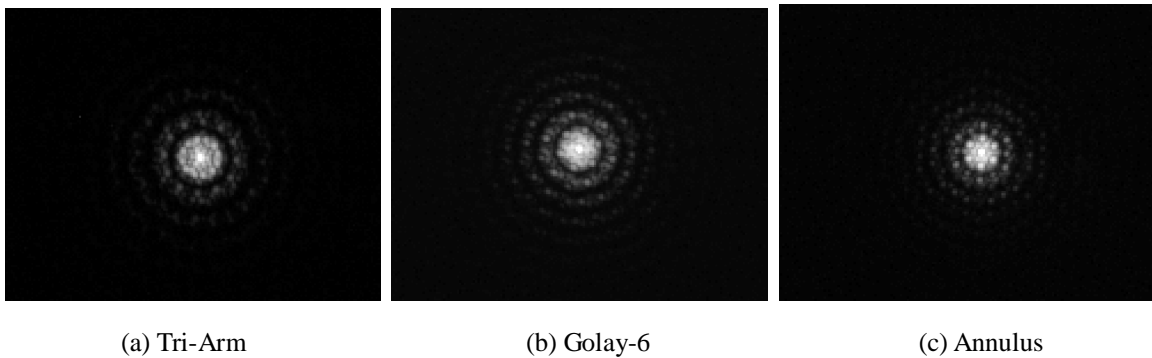


Fig.4 The measured PSFs of three typical array configurations

Compared with Fig.3, the difference between the measured PSFs and the calculated PSFs is not apparent, which means that after the fine adjustment the simplified optical sparse aperture system now have very little phase errors when combining the beams from the sub-apertures.

3) Imaging experiment with resolution target

In order to investigate the imaging capability of the optical sparse aperture system, a USAF 1951 resolution target is deployed into the experiment. The imaging experiment setup is illustrated in Fig.5. The source is a white light source output through a fiber. The wave filter's central wavelength is 532nm with a bandwidth of 10nm. The USAF 1951 resolution target is used to replace the pinhole in the forward focal plane of the achromatic doublet lens L_1 so as to simulate the remote extended target.

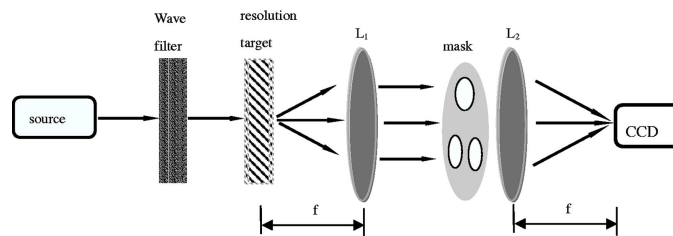


Fig.5 Setup of an optical sparse-aperture imaging system

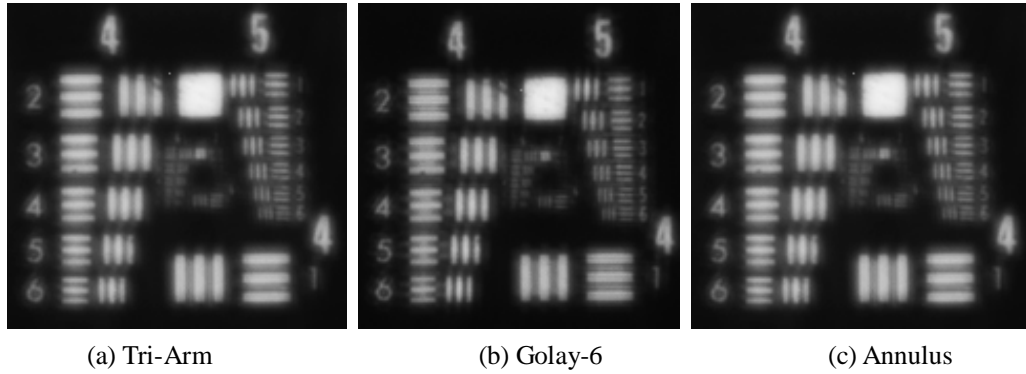


Fig.6 The resolution target imaging result

The original image is a 1317*1035 picture. In order to demonstrate the limit resolution of sparse aperture system, the high resolution portion in the picture is shown in figure 6. It is easily to recognize the 6th element of the 5th group, whose line width is $8.77\mu\text{m}$. The Golay-6 type mask even demonstrates the 1st element of 6th group which line width is $7.81\mu\text{m}$. As a comparison, the image of the equivalent filled aperture is illustrated in Figure 7. Without any post-process, the picture of equivalent aperture is much brighter than sparse apertures' because of the different light-collecting area. It is easy to distinguish the 1st element of 6th group whose line width is $7.81\mu\text{m}$, not like with Golay-6.

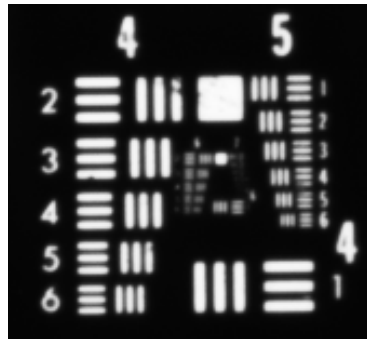
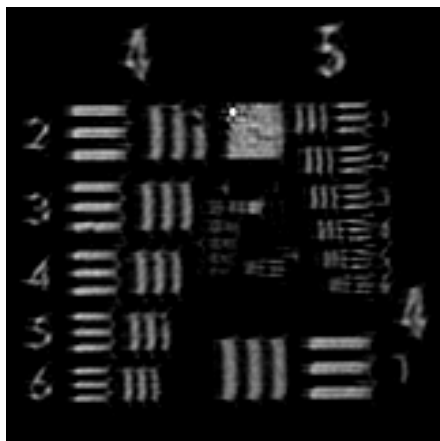


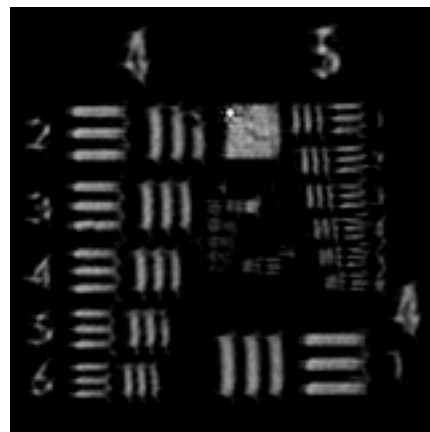
Fig.7 The resolution target imaging of equivalent aperture

4) Restoration of the sparse aperture system image

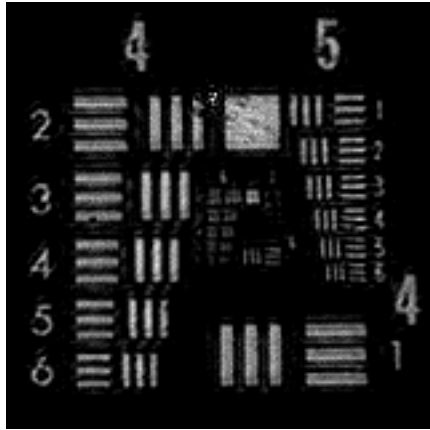
The Wiener filter needs the PSF as the parameter to deconvolve the image. The results are demonstrated in Fig.8.



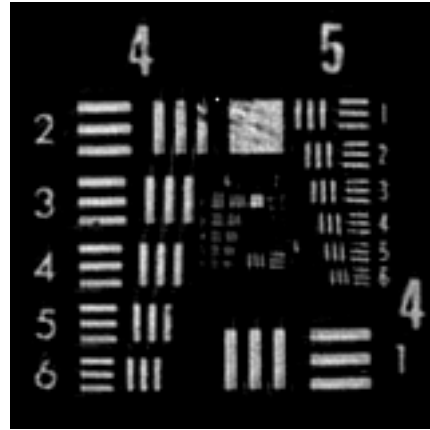
(a) Restored with the measured PSF



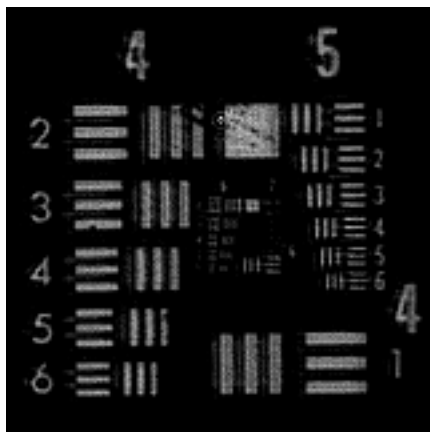
(b) Restored with the calculated PSF



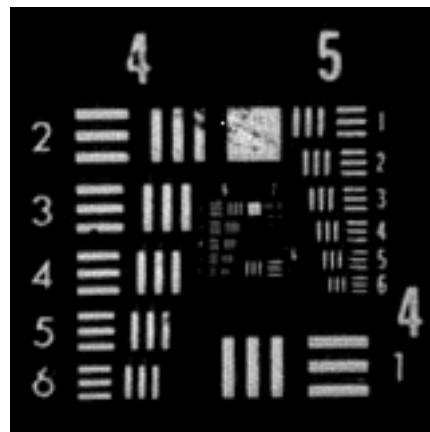
(c) Restored with the measured PSF



(d) Restored with the calculated PSF



(e) Restored with the measured PSF



(f) Restored with the calculated PSF

Fig.9 (a),(b) are the results of Tri-Arm mask. (c),(d) are the results of Golay-6. (e),(f) are the results of Annulus. The comparison illustrates clearly that with post-processing the resolution of optical sparse aperture system is improved largely. The previous work had already shown that, the higher filled factor was, the more frequency would pass the system[3]. Compared with the results from the measured PSF, the image restoration with the calculated PSF generates a more clearly picture. The explanation for the phenomena is that the PSF captured by the CCD contains the noise meanwhile there is still some little phase error between the combined beams. The detected image output directly from the optical sparse aperture system includes inherently the effect of the noise and the phase error. When restored with the measured PSF, the effect of the noise and the phase error on the measured PSF will interfere with the effect of the noise and the phase error on the direct image, and this will make the deconvolution process less perfect. In the worst case it even will introduce more blur into the picture. However, since the calculated PSF is clean, such interference does not appear, and the deconvolution process will produce much better results as long as the phase error is very small.

5. Conclusion

Based on the experimental results and analysis, the calculated PSF from telescope array configuration exhibits a more effective ability in retrieving the geometrical ideal image from the optical sparse aperture system. The measured PSF due to the noise and the residual phase error, is not suitable for Wiener filter used in post-processing of the optical sparse aperture system. If the phase error is small enough, the calculated PSF will work well for the

image restoration. In fact, to control the phase error is the most important key technique in the design of the optical sparse aperture telescope, because the light interfered in image plane is incoherent light. The calculated PSF is easier to obtain and more effective in the restored process. Possibly the measured PSF is no longer necessary for the sparse aperture system.

6. Acknowledgement

The authors acknowledge financial support from the Funding Project for Academic Human Resources Development in Institutions of Higher Learning Under the Jurisdiction of Beijing Municipality (PHRIHLB).

Financial support by the National Natural Science Foundation of China (NSFC) (Contract No.60577029), and partial financial support by The Science Foundation of Education Commission of Beijing, China (Contract No.KZ200910005001).

7. Reference

1. Soon-Jo Chung, David W. Miller, et al, "Design and Implementation of Sparse Aperture Imaging Systems", Proceedings of SPIE, Vol. 4849, 2002, p 181-192
2. Soon-Jo Chung, David W. Miller, et al, "ARGOS testbed: study of multidisciplinary challenges of future spaceborne interferometric arrays", Optical Engineering, Vol.43 (9) , 2004, p 2156-2167
3. Robert D. Fiete, Theodore A. Tantalos, Jason R. Calus, et al, "Image quality of sparse-aperture designs for remote sensing", Optical Engineering, 2002, Vol.41(8), p 1957-1969
4. Harvey J E, Kotha A, Phillips R L, "Image characteristics in applications utilizing dilute subaperture arrays", Applied Optics, 1995, Vol.34(16), p 2983~2992
5. Meinel A B and Meinel M P, "Large sparse-aperture space optical systems", Optical Engineering, 2002, Vol.41(8), p 1983~1994
6. R.L. Kendrick, Jean-Noel Aubrun, Ray Bell, et al, "Wide-field Fizeau imaging telescope: experimental results", Applied Optics, 2006, Vol.45(18), p 4235-4240
7. Dayong Wang, Ji Han, et al, "Experimental study on imaging and image restoration of optical sparse aperture systems", Optical Engineering, Vol. 46 (10) , 2007, p 103201
8. Nicholas J. Miller, Matthew P. Dierking, Bradley D. Duncan, "Optical sparse aperture imaging", Applied Optics, Vol. 46 (23) , 2007, p 5933-5943